Neuron, Vol. 37, 347–359, January 23, 2003, Copyright ©2003 by Cell Press

Basis Functions for Object-Centered Representations

Sophie Deneve[1] and Alexandre Pouget[2,*]
[1]Gatsby Computational Neuroscience Unit
Alexandra House
17 Queen Square
London WC1N 3AR
United Kingdom
[2]Brain and Cognitive Science Department
University of Rochester
Rochester, New York 14627

Summary

In an object-centered representation, the position of the subparts of an object are encoded with respect to a set of axes and an origin centered on the object. Several physiological and neuropsychological results support the existence of such representations in humans and monkeys. An explicit representation would involve neurons with invariant response properties in object-centered coordinates. We consider an alternative scheme using basis functions in which the cells have retinotopic receptive fields modulated by the orientation of the object and task-related signals. We show that this alternative is consistent with single-cell data, is computationally efficient, and accounts for object-centered hemineglect, a syndrome observed in humans after fronto-parietal lesions.

Introduction

The retinal image of an object changes whenever the object moves and every time the eyes move, either alone or as a result of head and body movements. Yet, our ability to recognize and manipulate objects is, to a large extent, independent of our posture in the environment as well as the position, orientation, and size of these objects. One possible explanation for this ability would be that cortical networks integrate sensory and postural inputs to create object-centered representations, i.e., a representation in which the position of the subparts of the object are encoded with respect to an origin and a set of axes centered on the object (Marr, 1982). The existence of such representations is supported by studies showing that attention can be allocated to specific locations within objects, regardless of their position and orientation (Duncan, 1984; Gibson and Egeth, 1994; Kahneman et al., 1992; Tipper et al., 1994).

Additional evidence comes from the study of patients with hemineglect, a neurological syndrome in which, following a lesion in their right cortical hemisphere, patients show a deficit in their ability to allocate attention to the left side of space (and vice versa, although right hemineglect tends to be rare). In particular, when asked to copy a drawing, neglect patients tend to ignore the left side of each object in the scene, whether the objects are seen in the left or right hemispace (Marshall and Halligan, 1993). This result is often interpreted as an object-centered form of neglect. However, it is possible that the behavior of the patients is the result of a competition between the right and left sides of the object, where left and right are defined in retinotopic coordinates, as opposed to object-centered coordinates (Driver et al., 1994; Driver and Pouget, 2000). To truly establish object-centered neglect, one must demonstrate that patients neglect the left side of an object regardless of its orientation.

Experiments that vary the orientation have typically found that neglect does not rotate with objects, i.e., patients keep neglecting the part of the object that is furthest to the left in *retinotopic* coordinates (Behrmann and Moscovitch, 1994; Drain and Reuter-Lorenz, 1997; Farah et al., 1990). This suggests that, for these experiments, what matters is the relative position of the subparts of the object, where position is defined in retinotopic coordinates, not object-centered (Driver and Pouget, 2000).

There are, however, a few experiments in which neglect has been reported to rotate with objects (Driver et al., 1994; Tipper and Behrmann, 1996). For instance, Driver et al. asked left hemineglect patients to detect the presence of a gap in the upper edge of an equilateral triangle (Driver et al., 1994). This triangle was surrounded by other equilateral triangles so as to form a figure that appeared tilted 60° clockwise or counterclockwise (Figure 1A). As a result, the upper edge of the target triangle appeared to belong to the left side of the overall figure in the clockwise condition, and to the right side in the counterclockwise condition. They found that neglect patients detected the edge more often when perceived to the right of the overall figure, thus showing an object-centered neglect dissociated from any retinotopic frame of reference.

Although such experiments support the existence of object-centered representations, they make no claims about the nature of these representations at the neural level. This issue is best addressed with neurophysiological experiments in monkeys as was done a few years ago by Olson and Gettner (1995). The authors trained monkeys to make a saccade to the right or left part of a bar while recording single unit activity in the Supplementary Eye Field (SEF). The protocol they used is presented in Figure 1B. The monkey had to fixate a central dot at the beginning of each trial. Next, a cue appeared at an irrelevant location to indicate to which side of the bar the saccade should be performed. The cue disappeared, and after a delay, a bar appeared at one of three possible contiguous locations at the top of the screen. As soon as the fixation point disappeared, the monkey had to make a saccade to the side of the bar that had been cued.

As shown in Figure 1C, some cells were found to be selective for a particular side of the object. For instance, the cell shown on the figure responded strongly prior to any saccade directed to the left side of the bar but only weakly to the same oculocentric saccades directed to the right side of the bar.

*Correspondence: alex@bcs.rochester.edu

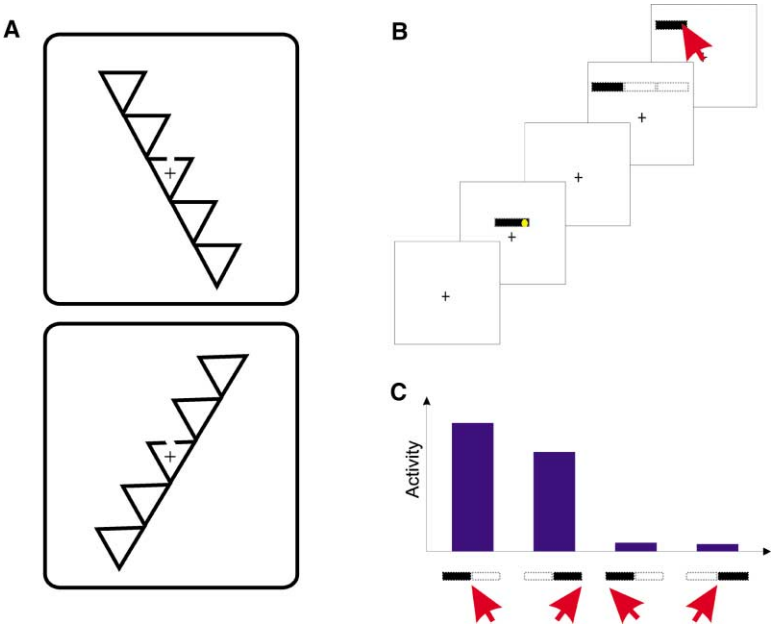

Figure 1. Experimental Results Supporting the Existence of Object-Centered Representations

(A) Driver et al. (1994) tested human patients with left hemineglect on a gap detection task. Patients were presented with either one of the two displays shown here. They were instructed to keep their eyes on the fixation point in the middle of the central triangle (indicated by the crosshairs). Their task consisted of detecting the presence of a gap that always appeared at the same retinal location, namely, on the edge directly above the fixation point. Previous experiments have demonstrated that these displays are perceived as being a horizontal set of triangles that have been rotated 60° clockwise (top) or counterclockwise (bottom). As a result, the gap is perceived to be on the left side of the figure in the top configuration and on the right for the bottom configuration. Driver et al. reported that patients tend to miss the gap more often when it appears to be on the left side of the figure (top), suggesting that neglect can be object-centered.

(B) Typical trial in Olson and Gettner's experiment (1995). The trial starts with the appearance of the fixation point. Next, a cue in the form of a bar appears with one side highlighed, instructing the monkey to move his eyes to the corresponding side when the target bar appears. After a blank screen, the target bar appears at one of three possible locations (dotted line). Finally, the fixation point disappears and the saccade is initiated.

(C) Response of a typical cell in the supplementary eye field between the appearance of the target bar and the initiation of the saccade. This cell shows object-centered selectivity because it responds strongly to saccades landing on the right side of the bar, but only weakly to saccades with the same amplitude and direction landing on the left side of the bar (compare conditions 1 and 3, and 2 and 4).

There are several possible interpretations for these results. For instance, the SEF may contain what we will call an *explicit* object-centered representation, that is to say, SEF neurons may have response fields centered on one particular part of the object regardless of its position, size, and orientation. Altogether, these neurons form a map in which the image of an object is repositioned, scaled, and rotated to represent the object in a "canonical" view (the map need not be topographic on the cortical surface). Such a representation has also been proposed to support view-invariant object recognition (Olshausen et al., 1995).

The goal of this paper is to present an alternative view, motivated by computational constraints and consistent with the neurophysiological data and the behavior of hemineglect patients. We argue that one of the purposes of object-centered representations is to facilitate the computation of motor commands whose goals are defined in object-centered coordinates. The task used by Olson and Gettner (1995) in which the monkey is instructed to saccade to a particular side of a bar is an example of such a command. In this case, the monkey is given an instruction and the image of a bar, and it must generate the appropriate eye movement command. This sensorimotor transformation requires an intermediate representation of the image and the instruction from which the motor command can be computed. We propose in this paper that this intermediate representation might involve a basis function map, a representation well suited to the computational nature of such tasks. Basis function maps represent all possible combinations of the sensory variables, so that linear combinations of them are sufficient to compute any motor commands, and in particular motor commands defined in object-centered coordinates such as "reach for the right side of the object."

Basis Functions versus Explicit Representations

In the task used by Olson and Gettner (1995), the monkey is asked to perform an eye movement based on an instruction and the image of a bar. The bar could appear in three possible locations and always in the same orientation. In this paper, we consider an extension of this task in which the bar can appear anywhere on the screen and in any orientation. We modified the original task because, as discussed in the introduction, rotating the object is essential for distinguishing object-centered from retinotopic representations.

As an example, consider a trial in which the monkey is instructed to make a saccade to the right side of a bar that has been rotated counterclockwise by 90°. In general, to foveate a target, the eyes must move by an amount equal to the retinal position of the target. Therefore, in order to perform the task properly, the monkey must recover the retinal position of the right side of the bar. One might think at first that we simply need to know the retinal location of all the subparts of the object and the current orientation of the object, but this is not quite sufficient. Just knowing that a particular subpart is located at $-10°$ horizontally and $+20°$ vertically on the retina, while the object is rotated by 90° counterclockwise, does not tell us where is this subpart within the object. However, if we are also told that this subpart lies on the top of the figure in retinotopic coordinates, we can now deduce that it must be the right side in object-centered coordinates. If, on the other hand,

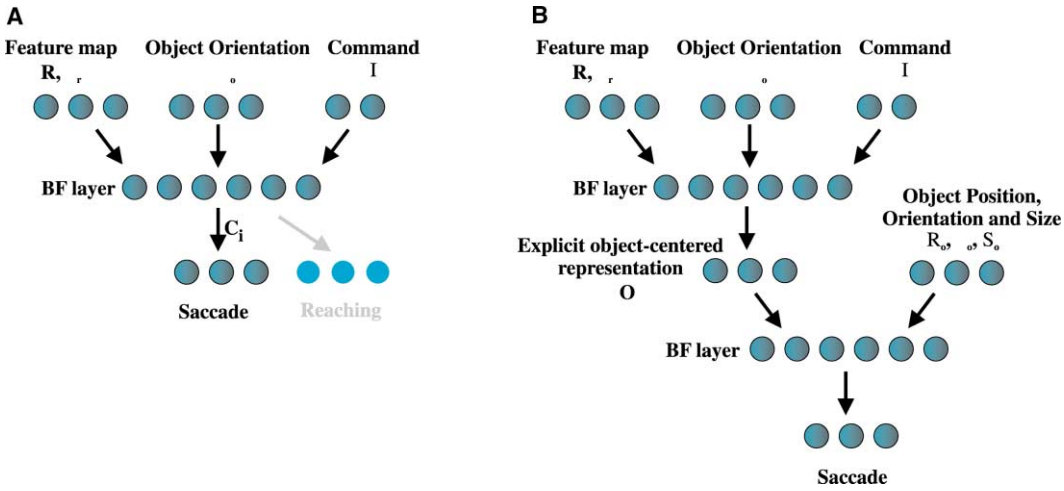

Figure 2. Neural Networks for Computing Object-Centered Saccades

(A) Sketch of a basis function network computing a saccade to a specified part of an object. This network has three layers: an input layer coding for the command I, θ_0, θ_R, and **R**, a basis function layer (BF layer), and an output layer specifying the saccade. The saccadic motor command can be obtained through a linear combination of the activities of BF units, with the appropriate set of coefficients c_i. Other output layers are indicated to emphasize the fact that the same BF layer can be used for other tasks.

(B) Same as in (A), but for a network using an explicit object-centered representation. The explicit representation cannot be computed directly from the input layers; it requires an extra step, which can take the form of a basis function layer, with inputs I, θ_0, θ_R, and **R**. Likewise, the saccade cannot be computed directly from the explicit representation, again requiring a basis function layer taking the explicit object-centered representation, the object's position on the retina R_0, orientation θ_0, and size S_0 as input. In other words, an explicit representation does not alleviate the need for basis functions and requires a minimum of five layers, as opposed to three for the basis function approach.

we are told that it lies at the bottom of the figure in retinotopic coordinates, we can conclude that this is the left side in object-centered coordinates. Therefore, the *relative* retinotopic coordinates of the subparts of the object are a critical piece of information.

This example shows that four critical pieces of knowledge are required to solve the task in general: (1) the instruction (e.g., go to the right side of the object), (2) the orientation of the object (e.g., 90° counterclockwise), (3) the *relative* retinotopic coordinates of the subparts of the object (e.g., is a particular edge on the top, bottom, right, or left side of the object in retinotopic coordinates?), and (4) the *absolute* retinal location of the subparts of the object (e.g., the location of the top edge on the retina).

In other words, the sensorimotor transformation involved in this task can be thought of as a mapping, or function, which takes as arguments the instruction (I), the orientation of the bar (θ_0), the *relative* retinal location of the subparts of the bar (θ_R), and finally, the *absolute* retinal location of the subparts of the bar (**R**). This function then returns the appropriate eye movement command (M). Note that we treat θ_R as a scalar and **R** as a vector. Indeed, θ_R is a variable that can take the values up (90°), down (270°), right (0°), and left (180°), while **R** is the location on the two-dimensional retina.

This scheme can be easily implemented in a three-layer network, as represented on Figure 2A. The input layers consist of groups of units encoding I, θ_0, θ_R, and **R**. The second layer is a basis function layer, in which units receive connections from the input units and compute basis functions of the input variables, $B_n(I, \theta_0, [\theta_R, \mathbf{R}])$. Here, the brackets $[\theta_R, \mathbf{R}]$ denote a list of absolute and relative retinal locations of the object's subparts. For example, if there are two subparts, the list contains six elements: the relative retinal location, as well as the horizontal and vertical absolute retinal location of the first subpart (three elements), and the same for the second subparts (three more elements). The third layer receives connections from the basis function units with weights, c_n, and computes the motor command M by taking a linear combination of the basis function units such that

$$M = f(I,\theta_0,[\theta_R,\mathbf{R}]) = \sum_{n=1}^{N} c_n B_n(I,\theta_0,[\theta_R,\mathbf{R}]). \quad (1)$$

The main claim of this paper is that neurons in the SEF or parietal cortex correspond to the basis function units.

There are several advantages to the basis function approach (Pouget and Snyder, 2000). First, once the activities of the basis function units are computed, the computation of a *nonlinear* function $f(I, \theta_0, [\theta_R, \mathbf{R}])$ reduces to a *linear* combination, a simple computation. Second, the same basis function units can be used for multiple transformations by connecting the basis function units to multiple output layers, encoding distinct motor commands. This makes this type of representation ideally suited for the coordination of multiple behaviors, such as moving the eyes, head, and hand toward the same side of an object. Third, learning is greatly simplified since any function can be obtained by adjusting the linear coefficients, which can be done with simple learning rules such as the delta rule or the covariance rule (Salinas and Abbot, 1995).

It is important to realize that not all representations are basis sets. In particular, an explicit object-centered representation, which would exclusively encode the ob-

ject-centered locations of the object subparts, **O**, does not provide a basis set for motor commands. In the case of eye movements, this is easy to see: you cannot move your eye to the right side of an object if you do not know where this right side is relative to your fovea. In addition to the object-centered location of the object subparts, one needs to know the current position, the orientation of the object on the retina, and its size. The transformation from the explicit representation to the motor command would therefore require an intermediate step such as a basis function representation of the object-centered location **O**, θ_0, the object position R_0, and size S_0.

In fact, the problem is even worse, because the computation of an explicit object-centered representation from a retinal image is highly nonlinear, requiring translation, scaling, and rotation of the image (Olshausen et al., 1995). As a consequence, it cannot be performed by a two-layer network (Bishop, 1995; Olshausen et al., 1995). Even if we start with inputs such as *I*, θ_0, θ_R, and **R** (as opposed to a raw retinal image), an intermediate representation is required to obtain an explicit object-centered representation, because the mapping is still nonlinear. In other words, while the basis function approach allows one to compute the motor command in a minimum of three layers, an explicit representation requires at least *five* layers (as sketched in Figure 2B): an input layer, a intermediate layer to compute the explicit object-centered representation, the explicit representation itself, another intermediate layer to compute the motor command from the explicit representation, and finally the motor command layer. One natural choice for the intermediate layers would be to use basis function representations. Therefore, explicit representations do not provide basis functions and are computationally less efficient since they require additional intermediate representations which themselves might involve basis functions.

Thus, our goal was to implement a network with an implicit object-centered representation like in Figure 2A to perform Olson and Gettner's task (1995) generalized to any object location and orientation. We used preprocessing stages to compute basis function representations of the absolute and relative retinotopic position of the subparts of an object, the object orientation, and the command. These basis functions were then used to implement the object-centered motor task. For the sake of biological realism, we used Gaussian basis functions, as detailed in the Experimental Procedures section. In the Results section we compare the response of the basis function units in our network with the results of Olson et al. (1995), and we show that lesions to this basis function representation lead to object-centered neglect without an explicit object-centered representation. These results have been presented in short form in Deneve and Pouget (1998).

Results

The network is divided into four layers: (1) an input layer, (2) a preprocessing layer, similar to V2, with edge detectors performing a rudimentary retinotopic segmentation, (3) a basis function layer corresponding to the parietal/premotor cortex where responses are modulated by the object orientation and the command, and (4) an output layer combining all responses from the parietal/premotor layer. The network structure is represented in Figures 3A and 7. The details of its architecture are described in the Experimental Procedures section.

This network is able to compute the goal of a saccade to an object (represented by a closed shape in the input layer) regardless of its position, size, shape, and orientation. Examples of activity patterns in the output layer for various orientations of the object are shown in Figure 3B.

Basis Function Layer

Figure 4A shows the activity of a parietal/premotor unit tested with two different saccade directions, two object orientations, and two commands. In this particular case, the cell responds best for a left-upward saccade directed to the right side of the object when the orientation of the object is 0°.

For comparison, Figure 4B shows what would be the expected response of a unit with a Gaussian response field in object-centered coordinates (Equation 5); that is to say, a unit belonging to an explicit object-centered representation. This specific unit would prefer any saccade directed to the right side of the object regardless of the position and orientation of the object. This response is difficult to distinguish from the basis function response if one only considers the conditions involving the object oriented at 0°—the conditions appearing in the dotted box in Figure 4. However, major differences arise when the object is shown at 180°. While the basis function unit fails to respond to any saccade in this condition (columns 4–8), the explicit unit would still respond to saccades ending on the right side of the object (column 4–5).

To further characterize the response of the basis function unit, we plotted its response field as a function of the retinotopic position of the object for the two possible instructions: go to the right and go to the left (Figure 4C). Like many cells in the visual cortex, the basis function unit shows a bell-shaped tuning to the position of the visual stimulus. In addition, the amplitude, or gain, of this tuning curve is modulated by the command and the orientation of the object.

Once again, the comparison with the explicit object-centered unit reveals major differences. In particular, an explicit object-centered unit would not show a bell-shaped tuning curve to the direction of the saccade, and the response would be insensitive to the orientation of the object (Figure 4D).

Thus, neurons in the basis function maps have the following properties: (1) they have retinotopic response fields, i.e., their response follows a bell-shaped function of the object position on the retina, just like many cells in premotor and parietal cortex (Andersen et al., 1990; Boussaoud et al., 1993; Schlag and Schlag-Rey, 1987), (2) the gain of these receptive fields is modulated by the command, and (3) the gain of these receptive fields is modulated by the orientation of the object in the view plane. Therefore, the parietal/premotor cells in our model do not have an invariant receptive field in object-centered coordinates.

This response pattern is consistent with the response of SEF cells recorded by Olson and Gettner (1995). In-

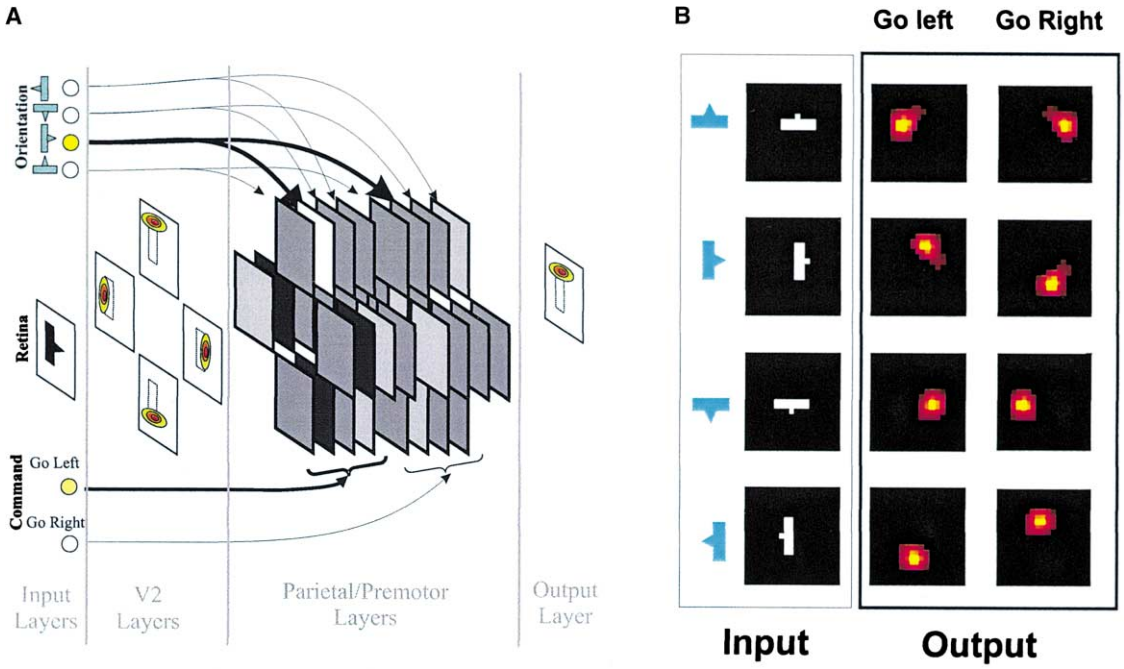

Figure 3. Network Architecture

(A) Schematic structure of the network and activation levels for the image shown on the left and the command "go to the right." The contour plots in the V2 and output maps represent the activity of the units. The parietal/premotor maps contain the basis function units. These maps are divided into compatible and incompatible maps (see main text). The compatible maps are shown in either light gray or white and send excitatory connections to the output layer. The incompatible maps are shown in dark gray or black and send inhibitory connections to the output layer. The parietal/premotor maps with the highest activity for the particular combination of the command and the object orientation illustrated here are the most contrasted: black for the most active incompatible map and white for the most active compatible map. The connections between the orientation and command layer onto the parietal/premotor layer modulate the gain of the visually evoked activity. The connections shown in bold correspond to the most active input units for the object shown here.

(B) Distribution of activity in the output layer for different positions and orientations of the figure and different commands. The figure consists of a bar with a triangle on top. The light gray drawings are the actual figures, while the adjacent black and white plots correspond to the digitized versions on the retina. Lighter shades of gray indicate more active units. In all cases, the network specifies the correct saccades, as indicated by the hills of activity centered on the correct side of the figure in all conditions.

deed, they tested only one orientation of the object and found that the response of some SEF neurons is selective to the position of the end point of the saccade in object-centered coordinates. This is exactly what we report for the basis function unit as can be seen by comparing Figure 1C and the conditions within the dotted rectangle in Figure 4A.

However, Olson and Gettner's results (1995) are also consistent with an explicit representation. In order to resolve this ambiguity, one would need to test the same neuron for various orientations of the object. Another test would be to map the response field of the neuron as a function of the direction of the saccade in retinotopic coordinates (as we did in Figure 4C for the basis function units). Sabes, Breznen, and Andersen (Sabes et al., 2002) have performed these experiments with monkeys while recording in the parietal lobe. Their results indicate that parietal neurons have retinotopic response fields modulated by the orientation of the object and the command, as predicted by our basis function hypothesis.

Lesion Experiment

If the basis function approach provides a correct formalization of the neural basis of object-centered representations, it should also account for object-centered hemineglect in humans. We show in this section that this is the case under the assumption that each hemisphere contains a retinotopic gradient and an object-centered gradient. The retinotopic gradient is such that each hemisphere mostly contains neurons with response fields on the contralateral hemiretina. The object-centered gradient is the consequence of an overrepresentation of units with specific pairs of preferred object orientation and relative retinal position in each hemisphere. Indeed, each combination of relative retinal position and object orientation corresponds to a particular object-centered location, even if the reverse is not true (an object-centered location does not specify the orientation of the object or a relative retinal position). For example, an object oriented at 0° and a relative retinal position of 0° (that is, an edge on the right of the figure in retinotopic coordinates) together specify the right part of the object, while an object orientation of 90° and a relative retinal position of 270° (that is, an edge on the bottom of the figure in retinotopic coordinates) together specify the left part of the object. We assume that cells preferring combinations of object orientation and relative retinal location specifying the right part of an object are more numerous in the left hemisphere, while units with combinations of selectivity specifying the left part of an

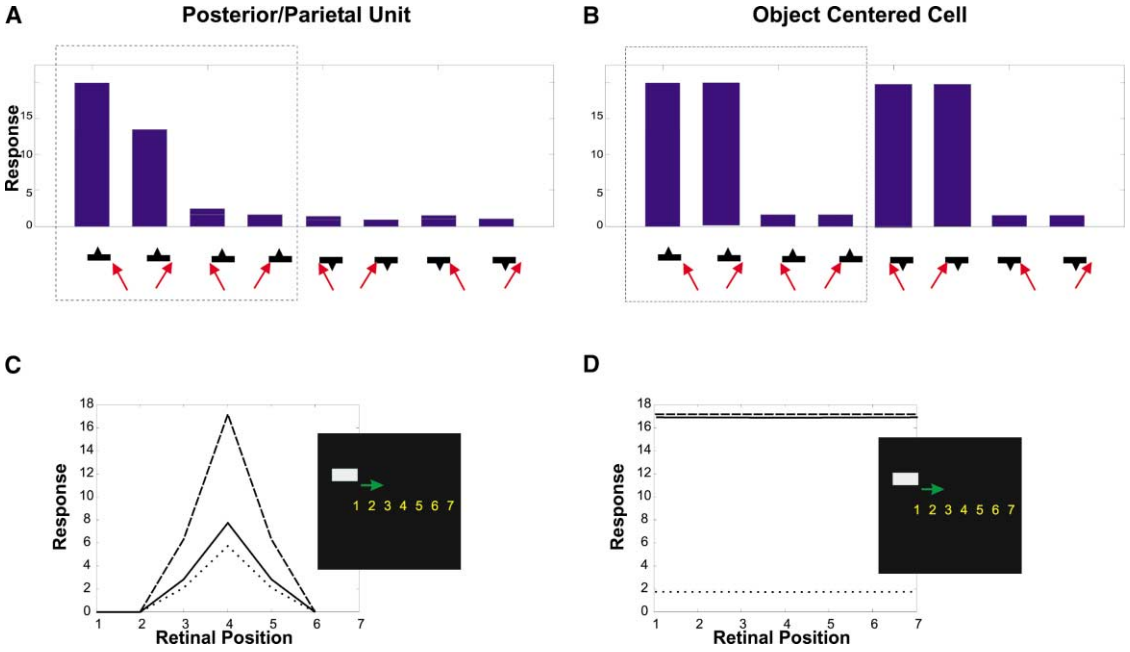

Figure 4. Response of a Typical Parietal/Premotor Unit and Comparison with a Unit in an Explicit Object-Centered Representation

(A) Histograms representing the activity of a typical parietal/premotor cell for two different saccade orientations, two different commands, and two different object orientations, as indicated by the sketches below. The conditions circled with dotted lines are the ones tested by Olson and Gettner (1995).

(B) Same as in (A) but for a unit in an explicit object-centered representation. Clearly, the conditions tested by Olson and Gettner hardly differentiate between a basis function unit and an explicit object-centered unit.

(C) Activity of a parietal/premotor unit as a function of the stimulus position. Dashed line: command "go right," object orientation 0°. Solid line: "go right," orientation 90°. Dotted line: "go left," orientation 0°. This unit has a retinotopic receptive field whose amplitude, or gain, is modulated by the orientation of the stimulus and the command.

(D) Same as in (C) but for a unit in an explicit object-centered representation. This type of unit does not show any selectivity to the retinal position of the stimulus.

object are more numerous in the right hemisphere. This creates a hemispheric gradient that appears to be object-centered even if it does not involve cells with invariant object-centered receptive fields (see Experimental Procedures for details regarding the implementation).

In the first set of simulations, we investigated the effect of a complete lesion of the right hemisphere on the performance of the network in the generalized Olson and Gettner's task (1995). For clarity, we start by describing the results for a network containing *only* the object-centered gradient. As one might expect, the damaged network is now unable to perform any saccade directed to the left side of the object regardless of the position and orientation of the object, while being completely spared for saccades directed to the right side (Figures 5A and 5B). Interestingly, this impairment generalized across any orientation and any position of the bar. In other words, the network shows a pure form of left hemineglect in object-centered coordinates.

Next, we simulated a lesion in a network with both the retinotopic and object-centered gradients (see Experimental Procedures). This intrahemispheric retinotopic gradient is known to exist in human and nonhuman primates (Ben Hamed et al., 2001; Lagae et al., 1994; Tootell et al., 1998). The network is now impaired for saccades directed to the left hemiretina and to the left of objects (Figures 5C and 5D). Even when the saccade is directed toward the right part of the object, the activity on the SEF is much weaker for saccades to the left in retinotopic coordinates, which might result in a failure to trigger an accurate saccade or in a slower reaction time. Therefore, hemineglect affects a mixture of the object-centered and retinotopic frames of reference. Preliminary data from Olson and Gettner (personal communication QA) show that a lesion of the parietal lobe leads to a similar deficit in which the impairment affects both frames of reference. Moreover, this mixture of frames of reference is also found in hemineglect patients (Behrmann and Tipper, 1999). Indeed, to our knowledge, patients with object-centered neglect always show retinotopic neglect as well. Note that these data would be difficult to reconcile with an explicit representation since a lesion restricted to an object-centered area would predict pure object-centered neglect with no retinotopic component.

Next, we tested our network on the Driver et al. experiment illustrated in Figure 1A. This experiment required patients to detect the presence of a gap in the upper edge of the middle triangle. Our network was not designed to perform this task, but one of the advantages of the basis function representation is that it is not task specific and can be used for any sensorimotor task involving the object. In this particular situation, we assumed that the activity in the basis function map influences the patients' performance.

More specifically, we propose that the performance

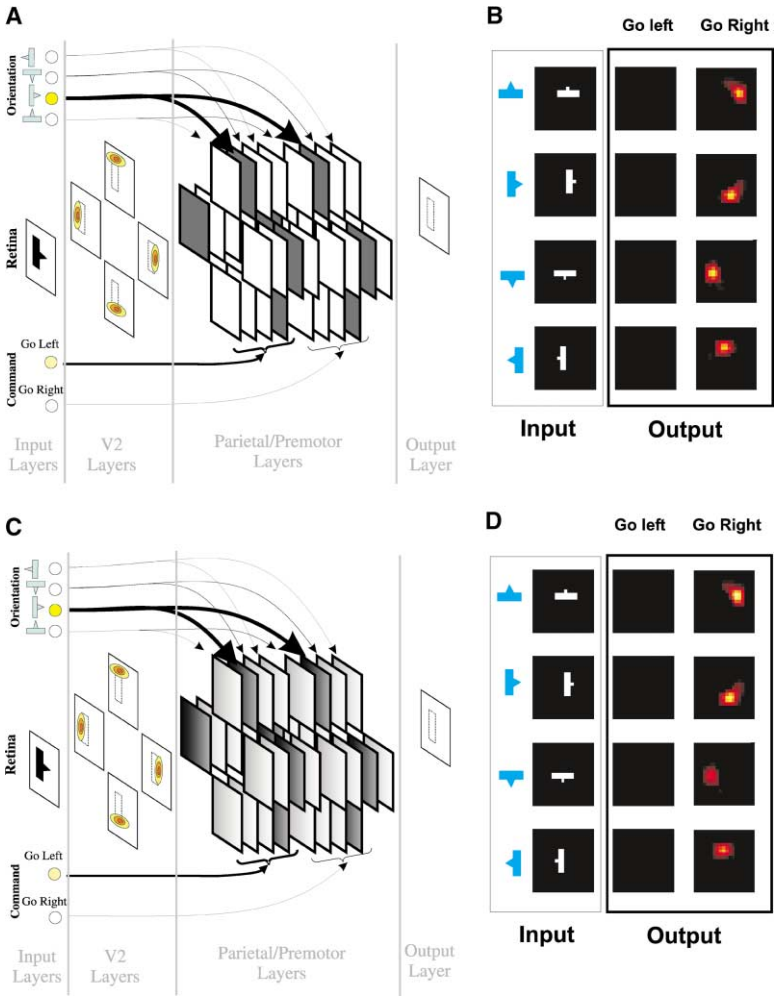

Figure 5. Effect of a Unilateral Hemispheric Lesion on Network Performance

(A) Network with a pure object-centered lesion. The activity of the parietal/premotor layers indicated in gray has been decreased to mimic the effect of a lesion.

(B) Activity in the output layer of the network with a pure object-centered lesion. The network performs normally for saccades directed toward the right of the object, while failing completely for saccades directed to the left side.

(C) Network with a mixture of an object-centered and retinotopic lesion. The gray level indicates the severity of the lesion in the parietal/premotor maps. All maps are damaged along the horizontal retinal dimensions, with the left side being the most damaged. Moreover, in the maps associated with the left side of the figure, the lesion is even more severe (darker maps), corresponding to the object-centered components of the lesion.

(D) Activity in the output layer of the network with a mixture of object-centered and retinotopic lesions. The network cannot generate saccades directed to the left side of the object, and it shows reduced activity for saccades directed toward the left hemiretina, even when the saccade ends on the right side of the object (third condition from top, right image). The deficit is both retinotopic and object-centered.

of the patients is proportional to the saliency of the upper edge, where saliency is defined as the sum of the basis function units responding to the upper edge across all maps. The notion that activity in the parietal cortex corresponds to the saliency of the object, or a subpart thereof, is strongly supported by single-cell recordings (Gottlieb et al., 1998) and the study of hemineglect patients. We are simply extending this notion to the case of object-centered representations.

As we did before, we considered two types of hemispheric gradients: a pure object-centered gradient and a combination of object-centered and retinotopic gradients. In both cases, we presented a digitized version of the central triangle on the retina while the orientation input units were set to represent the perceived orientation (60° clockwise or counterclockwise) provided by the alignment of all the triangles. The command units are ignored altogether in this task since they play no role. The consequences of a simulated lesion of the right hemisphere are very similar in both conditions. As can be seen in Figure 6, the saliency of the upper edge decreases when it is perceived as belonging to the left side of the object versus the right side.

This predicts that patients should perform better when the upper edge is perceived to belong to the right side, which is indeed what was reported by Driver et al. The source of this effect can be attributed to the orientation input. Among the units selective to the upper edge, the ones that are most affected by the lesion are those receiving a strong input from the input units tuned to an orientation of 60° clockwise, because they are the ones selective to the left side of objects. As a result, the overall activation in the basis function map in response to the upper edge is greatly reduced when the object is tilted 60° clockwise compared to 60° counterclockwise. When the lesions also affect the retinotopic dimension, the deficit is exacerbated by the fact that the right edge of the triangle (right in retinotopic coordinates) is much more salient than the upper edge when the object is rotated 60° clockwise, simply because the retinal gradient favors rightward positions. In other words, the upper edge is not salient and lies next to a salient edge that is likely to attract the patient's attention.

We emphasize that the results of our simulation of the Driver et al. experiment do not depend of the exact profile of the hemispheric gradients. All that is needed is that the top or bottom features (in retinotopic coordinates) are differentially activated by the perceived clockwise or counterclockwise orientation.

To summarize, the basis function approach can easily account for object-centered neglect in both motor and

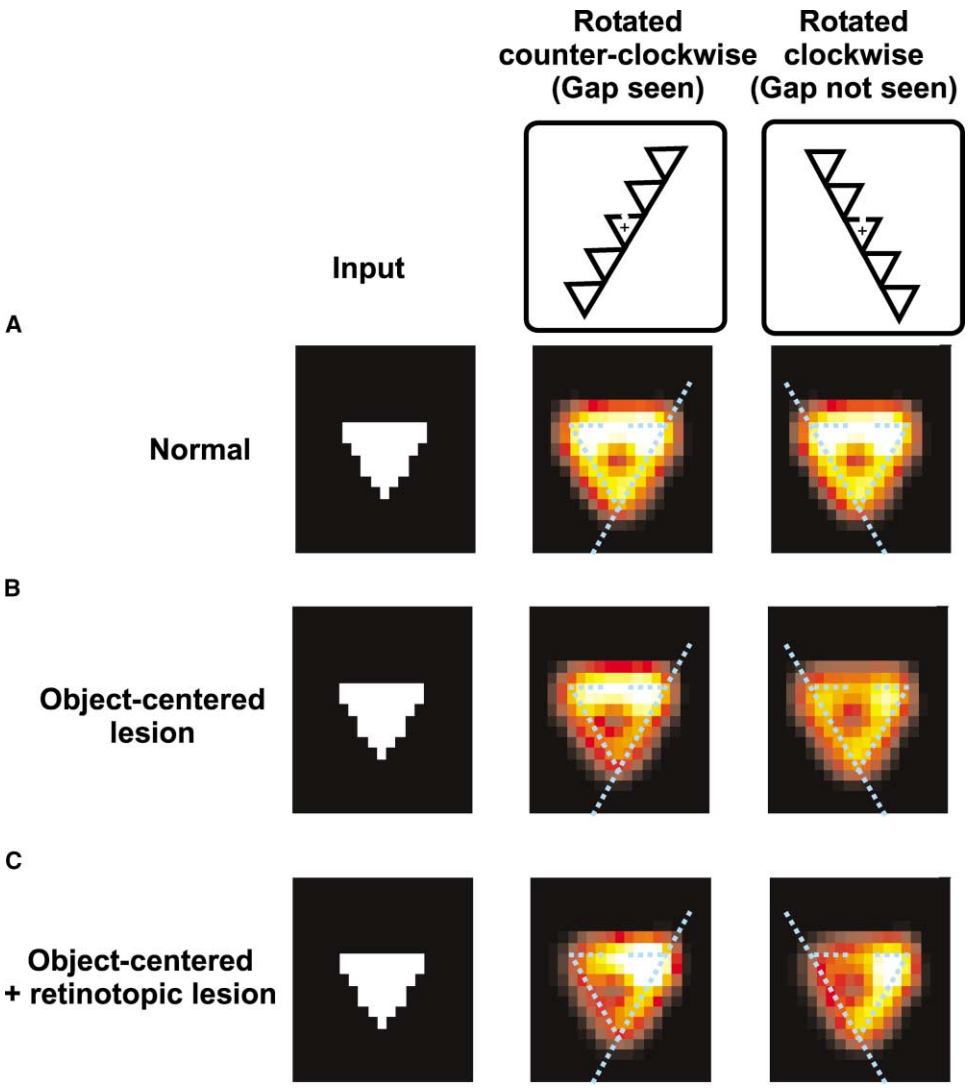

Figure 6. Activity in the Network's Output Layer in the Experiment of Driver et al.

The left column shows the digitized image of the central triangle as seen on the retina. The central and right columns show the activity evoked by the central triangle when the object is rotated counterclockwise (Figure 1A, center, bottom) or clockwise (Figure 1A, right, top). The dotted line outlines the contour of the triangle and its perceived orientation.

(A) Network with no lesion.

(B) Network with a pure object-centered lesion. The activity is stronger for the edge perceived to be on the right side of the figure. This predicts that a gap in the upper edge is easier to detect in the center condition, which is indeed what Driver et al. reported for left hemineglect patients.

(C) Network with a mixture of eye-centered and object-centered lesions. Edges perceived to be on the right side of the figure still evoked the strongest activity, but within the edges themselves, the eye-centered right side evokes more activity. The middle of the upper edge is still more salient in the central condition, which is also consistent with Driver et al.'s results.

sensory tasks. Furthermore, this approach can also explain why hemineglect affects a mixture of retinotopic and object-centered coordinates. This latter result requires the existence of a contralateral retinotopic gradient in each hemisphere, which is known to exist in the parietal lobe of monkeys and humans (Ben Hamed et al., 2001; Tootell et al., 1998).

Discussion

The main conclusion of this study is that object-centered representations in the brain appear to involve basis function maps as opposed to explicit representations. The advantages of the basis function approach are three-fold. First, basis functions provide a robust computational solution for implementing object-centered sensorimotor transformations in a neural architecture. Second, the tuning of the basis function units is consistent with the response of single cells in the SEF and parietal lobe. And third, a lesion of a basis function representation accounts for object-centered neglect and the fact that it is always mixed with retinotopic neglect.

By contrast, the hypothesis that object-centered rep-

resentations are explicit fails on all three counts: it is less efficient for sensorimotor transformations in the sense that it would require additional layers of processing compared to basis functions; it does not fully account for the response properties of parietal cells; and it predicts pure object-centered neglect, a behavior which has never been reported despite numerous reports of other double dissociations in hemineglect patients. This is not to say that explicit representations do not exist in the brain. Other cortical regions, beside the posterior parietal cortex, might contain such representations. In fact, the SEF might even be such a region since the published data do not allow us to distinguish between an explicit object-centered representation and basis functions.

One of the main drawbacks of the basis function approach is known as the curse of dimensionality: the number of basis functions required to approximate functions with high accuracy increases exponentially with the number of signals being combined (Poggio, 1990). Using an explicit representation is unlikely to solve this problem, unless there exists a way to obtain an explicit representation without using basis functions—which remains to be shown. The standard solution instead is to break down the problem into intermediate computations involving a subset of the variables.

Interestingly, this weakness of the basis function approach is also one of its main strengths. Because it uses so many units, a basis function representation tends to be highly redundant. This redundancy can be exploited to filter out the noise optimally. We worked with noiseless neurons in this study, but in reality, cortical neurons exhibit spontaneous activity and high variability in their spikes trains (Gershon et al., 1998; Tolhurst et al., 1982). This variability can be filtered out optimally in a basis function network by adding lateral and feedback connections and tuning them appropriately (Deneve et al., 2001).

Object-Centered Hemineglect

Our simulations of object-centered neglect relied on the assumption that basis function units are distributed across hemispheres according to a retinotopic and object-centered gradient. The existence of the retinotopic gradient is supported by recordings in the SEF and parietal lobe showing that each hemisphere overrepresents the contralateral retina. The gradient along the object-centered dimension has not been as extensively studied but preliminary evidence also supports our assumption. Thus, Olson and Gettner (1995) reported that within each hemisphere, most cells tend to prefer the contralateral side of the bar. Reuter-Lorenz et al. (1996) also reported the existence of a hemispheric object-centered attentional bias in normal subjects: subjects were better at detecting a small gap on the right side of a square presented on the right, or on the left if the square was presented on the left, compared to a gap on the other side of the object but at the same retinotopic location. They interpreted this result as a hemispheric attentional bias for the contralateral side of objects (Reuter-Lorenz et al., 1996).

Our account of object-centered neglect relies on the existence of an object-centered representation using basis functions. In contrast, Mozer (1999) has argued that the results of Driver et al. (1994), illustrated in Figure 1, can be explained without invoking the existence of any kind of object-centered representation. In his model, the effect appears as the consequence of the dynamics of activation of a retinotopic saliency map. Therefore, it is possible that the results of Driver et al. do not provide definitive evidence for the existence of object-centered representations.

However, it remains true that humans and monkeys alike can reach or move their eyes to a specific side of an object, regardless of the position and orientation of the object. Moreover, the presaccadic response of SEF and parietal neurons is clearly conveying information related to the object-centered locations of the subparts of objects (Sabes et al., 2002). A purely retinotopic model, as used by Mozer (1999), cannot account for these facts, hence the need for a unifying framework, as provided by the basis function approach.

Generality of the Basis Function Approach

The basis function approach is not specific to object-centered representations and has been successfully applied to other problems. Pouget et al., for instance, have argued that spatial representations used for egocentric sensorimotor transformations, such as reaching for an object, involve basis functions of the visual inputs and the signals related to the posture of the body (Pouget et al., 1999; Pouget and Sejnowski, 1997, 2001). The basis function they used consisted of neurons with bell-shaped retinotopic receptive fields whose amplitude was modulated by signals encoding the position of the eyes and head. This multiplicative interaction between a sensory response and a posture signal is sometimes called a gain field, a response pattern that has been reported throughout the parietal lobe and premotor cortex (Pouget and Snyder, 2000).

The alternative to basis functions in this context would be to use explicit representations in head-centered or body-centered coordinates. Neurons with invariant response fields in head-centered or body-centered coordinates have been found in the parietal lobe but in surprisingly small numbers (Duhamel et al., 1997; Galletti et al., 1993), suggesting once again that basis functions are the favored type of representation. In fact, it is possible that the explicit neurons are modulated by other posture signals that were not tested in these experiments, in which case they would constitute basis functions as well.

Object recognition is another computational domain in which explicit and basis function representations have been discussed as possible alternatives. Olhausen et al., for instance, have proposed a shifter circuit that can compute an explicit object-centered representation from the retinal image of an object (Olshausen et al., 1995). By contrast, Poggio et al. have argued that object recognition can be formalized in terms of nonlinear mappings and can therefore be implemented in a basis function network (Poggio, 1990; Riesenhuber and Poggio, 1999).

Current neurophysiological evidence appears to favor the basis function hypothesis. There has been no report of neurons responding to the position of the subpart of an

object in object-centered coordinates. Instead, neuronal responses in the inferior temporal cortex show a specificity to the shape of objects, or part thereof, modulated by the retinal location of the object and its angle of view (Logothetis and Pauls, 1995; Logothetis et al., 1995; Wachsmuth et al., 1994). As shown by Poggio et al., these responses are precisely what would be expected in a basis function network for object recognition.

These are only a few examples of domains in which the basis function approach accounts for the response properties of cortical neurons. One advantage of basis function representations is that they can be easily combined. For example, our basis function units could also be modulated by eye position. In this case, they could be used simultaneously to perform object-centered and head-centered tasks and could be said to represent implicitly, and simultaneously, eye-centered, head-centered, and object-centered positions. Given the high degree of similarity of the cortical architecture between areas such as the prefrontal cortex, infero-temporal cortex, and parietal lobe, one would expect that some computational principles are shared throughout the cortex, and we believe that a basis function representation could be one of them.

Experimental Procedures

Basis Function Representations

Performing the Olson and Gettner's task amounts to computing the function f such that $M = f(I, \theta_0, [\theta_R, \mathbf{R}])$ where $[\theta_R, \mathbf{R}]$ correspond to a list of all relative and absolute locations of the object's subparts. With the basis function approach, this task is decomposed into two steps. In the first step, intermediate neurons compute basis functions of the input variables, in this case, I, θ_0, θ_R, and $\mathbf{R}$. In the second step, the basis functions are combined linearly to recover the function $f(I, \theta_0, [\theta_R, \mathbf{R}])$. In other words, the function, $f(I, \theta_0, [\theta_R, \mathbf{R}])$, is approximated as a linear combination of the basis functions $B_n(I, \theta_0, [\theta_R, \mathbf{R}])$:

$$M = f(I,\theta_0,[\theta_R,\mathbf{R}]) = \sum_{n=1}^{N} c_n B_n(I,\theta_0,[\theta_R,\mathbf{R}]). \quad (2)$$

The weights c_n can be found with a standard linear regression procedure or with a learning rule such as the delta rule (Moody and Darken, 1989; Pouget and Sejnowski, 1997; Salinas and Abbot, 1995).

There are many families of functions, $B_n(I, \theta_0, [\theta_R, \mathbf{R}])$, that can be used as basis functions. For instance, one could choose sine functions of I, θ_0, θ_R, and $\mathbf{R}$ with all possible frequencies and phases. That is to say, one could use a large number of intermediate neurons whose receptive fields to I, θ_0, θ_R, and $\mathbf{R}$ follow cosine profiles with frequencies and phases specific to each unit. The function $f(I, \theta_0, [\theta_R, \mathbf{R}])$ would then be expressed as a sum of cosine functions. This particular decomposition is better known as a Fourier transform and the appropriate coefficients c_n are the Fourier coefficients for $f(I, \theta_0, [\theta_R, \mathbf{R}])$. A Fourier transform is indeed one example of how a function can be expressed as a sum of basis functions.

In this paper we consider another family of basis functions, namely functions of the form:

$$B_n(I,\theta_0,\theta_R,\mathbf{R}) = H_n(I)G_n(\theta_0)G_n(\theta_R)G_n(\mathbf{R}), \quad (3)$$

$$= H_n(I)\exp\left(-\frac{(\theta_0 - (\theta_0)_n)^2}{2\sigma_{\theta_0}^2}\right)\exp\left(-\frac{(\theta_R - (\theta_R)_n)^2}{2\sigma_{\theta_R}^2}\right)\exp\left(-\frac{\|\mathbf{R} - \mathbf{R}_n\|^2}{2\sigma_R^2}\right), \quad (4)$$

where $H_n(I)$ is a modulation by the instruction I (e.g., it is maximum for one particular command specific to unit n, and near zero for all other commands) and $G_n(x)$ stands for a Gaussian function of x. We assume that the Gaussian function for θ_R and $\mathbf{R}$ are narrow relative to the size of the object, such that only one subpart of the object falls within the receptive field of a given unit. Therefore, we can replace the notation $[\theta_R, \mathbf{R}]$ with θ_R, $\mathbf{R}$, since the list is reduced to one item per unit.

This equation corresponds to a neuron with a Gaussian retinotopic receptive field centered on position $\mathbf{R}_n$ whose amplitude is modulated by the instruction, the orientation of the object, and the relative retinotopic position of the subpart of the object falling in its receptive field (we assume that the receptive field of the neuron is small enough so that only one object subpart can fall in its receptive field). σ_{θ_0}, σ_{θ_R}, and σ_R are parameters that control the width of the tuning curves, while $(\theta_0)_n$, $(\theta_R)_n$, and $\mathbf{R}_n$ are the preferred values for unit n for the corresponding variables. As shown in the Results section, this particular choice provides a good fit to neurophysiological data.

Note that an explicit object-centered representation does not provide a basis function map for the task we are considering here. The issue is whether one can compute the motor command—a function that depends on I, θ_0, θ_R, and $\mathbf{R}$—from a set of functions that depend exclusively on the object-centered coordinates of the target, $\mathbf{O}$. For instance, consider a family of neurons with Gaussian receptive fields in object-centered coordinates. These neurons' responses, a_n, would follow:

$$a_n = \exp\left(-\frac{(\mathbf{O} - \mathbf{O}_n)^2}{2\sigma^2}\right), \quad (5)$$

where $\mathbf{O}_n$ is the preferred object-centered location of neuron n. A family of such functions cannot be combined linearly to compute an eye movement command because three variables are missing, namely, the object position on the retina R_0, orientation θ_0, and size S_0.

Network Architecture

The input layers of the network consist of three groups of units. The first group of two units encodes the instruction, I, provided by the cue, i.e., move to the right or to the left. The second group provides a distributed representation of the orientation of the object, θ_0. It involves four units with bell-shaped tuning curves and preferred orientations of 0°, 90°, 180°, and 270°, respectively. These units are similar to neurons in the inferotemporal cortex (Logothetis and Pauls, 1995) and the intraparietal sulcus (Sakata et al., 1998), which are tuned to the orientation of objects in the view plane. The third group of units forms a 29×29 retinotopic map, similar to the maps found in the early stages of the visual system. The activity of these units is proportional to the luminance in the image.

The goal of the next layer—the preprocessing layer—is to create maps of units simultaneously encoding the *absolute* and *relative* retinotopic coordinates of edges appearing in their receptive fields (noted $\mathbf{R}$ and θ_R, respectively). Recall that these two variables are needed for the computation of the object-centered saccade (see Introduction). We used four retinotopic maps, corresponding to four relative retinotopic positions: top, down, right, and left. Thus, in the top map, units responded to a vertical edge only if it appeared in the unit's receptive field and the edge belonged to the top side of the bar, but not if it belonged to the bottom side (where top and bottom are meant in retinotopic coordinates). We will refer to this layer of the network as the V2 layer because neurons with such selectivity have been reported in area V2 (Zhou et al., 2000).

In our network, this selectivity emerged as a result of using odd Gabor filters with four orientations: 0°, 90°, 180°, and 270°. Each filter was characterized by a 10×10 kernel (as shown in Figure 7A). The activity in each of the four maps was obtained by convolving the 29×29 retinotopic input map with one particular filter, resulting in four 20×20 maps. For instance, the activity of a unit located at position ij on map k (where k can take the values 1 to 4 corresponding to right, up, left, and down) is:

$$V_{ij}^k = \left[\sum_{l=1}^{10}\sum_{m=1}^{10} W_{l,m}^k U_{l+i-1,m+j-1}\right]^+ \quad (6)$$

where W^k is the kernel for map k and $U_{l,m}$ is the activity of the unit at position l, m on the retina, and where:

$$[x]^+ = \begin{cases} x & \text{if } x>0 \\ 0 & \text{otherwise} \end{cases}. \quad (7)$$

Similar equations were used in the other maps, and the resulting distribution of activity on the V2 layers for bar or triangle objects is

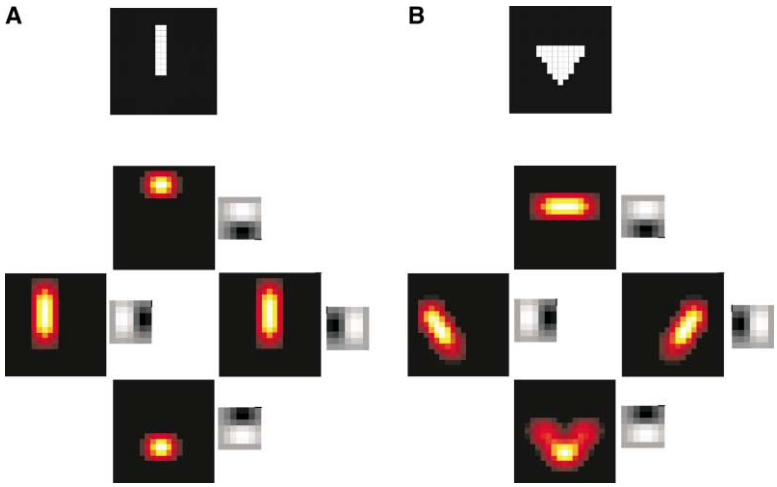

Figure 7. Segmentation of the Figure by the Four V2 Maps

(A) Segmentation of a vertical bar. The top image represents the input on the retina. The four bottom images represent the activity level in the four V2 maps, along with the filter used to compute these responses. These maps are meant to compute the relative retinal locations of the subparts of the object.
(B) Same as in (A) but for a triangle.

plotted in Figure 7. These equations lead to units with bell-shaped tuning curves to the relative and absolute retinal position of the edges of objects. In other words, and to a first approximation, the activity of any V2 unit in response to an edge appearing at the retinal position $\mathbf{R} = (I, m)$ and with relative retinal location θ_R can be rewritten as the product of two Gaussian tuning curves:

$$V_{ij}^{k} = G_k(\theta_R)G_{ij}(\mathbf{R}), \tag{8}$$

$$= \exp\left(-\frac{(\theta_R - \theta_R^k)^2}{2\sigma_{\theta_R}^2}\right)\exp\left(-\frac{(I - i)^2 + (m - j)^2}{2\sigma_R^2}\right), \tag{9}$$

where θ_{Rk} is the preferred relative retinal location of the unit and $\mathbf{R}^k_{ij} = (i, j)$ is its preferred absolute retinal location. This approximation becomes particularly helpful when we describe the activity of the basis function units.

Using odd Gabor filters is clearly insufficient to endow the units with a selectivity to relative retinal position that is invariant across a wide range of objects. However, it is sufficient for the objects used in this model, i.e., black figures with convex shapes on white background. This part of the model could be developed further to deal with other objects, but this would not impact our theory of object-centered representations while making the model significantly more complex.

The third layer of the network, meant to model the parietal/premotor cortex, combines the activity from the V2 layer with signals coming from the input layers encoding the orientation of the objects and the command. This part of the network computes basis functions of the four variables required to solve the task: the command (I), the orientation of the object (θ_o), the relative retinotopic locations of the subparts of the objects (θ_R), and their absolute retinal locations ($\mathbf{R}$). This layer is divided into four groups of retinotopic maps, each group receiving one-to-one connections from a corresponding map in V2. For instance, within the top group all cells respond preferentially to a horizontal edge located on the top part of the object (in retinotopic coordinates).

Within each group, the retinotopic maps differ by their selectivity to the command and the orientation of the object. Thus, each of the four edge-selective groups contains eight maps, resulting in a total of $4 \times 8 \times 20 \times 20 = 12800$ basis function units. Each unit in the first four maps receives a connection from the input unit encoding the command "go to the right," while units in the other four maps receive a connection from the input unit encoding the command "go to the left."

These eight maps are also modulated by the orientation of the object: The first and fifth maps are maximally activated by an orientation of 0°, the second and sixth map by an orientation of 90°, the third and seventh by an orientation of 180°, and the fourth and eighth by an orientation of 270°. Thus, in the 32 parietal/premotor maps, all possible combinations of feature selectivity (vertical right, vertical left, horizontal top, and horizontal bottom edge), object orientation selectivity (0°, 90°, 180°, or 270°), and command selectivity ("go to the right" or "go to the left") are represented. The modulation by object orientation is gradual: it follows a bell-shaped function of the difference between the preferred orientation of the unit and the orientation of the object. For example, an object orientation of 180° leads to a maximal amplification of the 180° selective maps and a maximal suppression of the 0° selective maps, and intermediate levels of modulation for the 90° selective and 270° selective maps. This ensures that the intermediate representation we use can deal with intermediate orientations that are not explicitly represented in the cell's preferences (for example, an object oriented at 45°). The modulation by the command is simply a multiplication by 1 when the command unit connected to the map is active, and by 0.3 otherwise.

As a consequence, parietal/premotor cells have retinotopic response fields modulated by the orientation of the object and the command. All these modulations are multiplicative. Thus, the activity of a parietal/promotor cell ij in the map selective to 90° orientation and the command "go to the left" in the group responding to top edges is:

$$P_{ij}^{k,l,m} = H_m(I)G_l(\theta_0)V_{ij}^{k}, \tag{10}$$

where

$$G(\theta_0) = \exp\left(-\frac{(\theta_0 - (\theta_0)_I)}{2\sigma_{\theta_o}^2}\right) \tag{11}$$

and

$$H_m(I) = \begin{cases} 1 & \text{if } I = m \\ 0.3 & \text{otherwise} \end{cases}. \tag{12}$$

Using the approximation shown in Equation 8, Equation 10 can be rewritten as:

$$P_{ij}^{k,l,m} = H_m\,(I)G_l(\theta_o)V_{ij}^{k}, \tag{13}$$

$$= H_m(I)G_l(\theta_o)G_k(\theta_R)G_{ij}(\mathbf{R}). \tag{14}$$

This equation is identical to Equation 3 in the previous section; the only difference is that the index n is now a five-dimensional vector k, l, m, i, j. This shows that the response of these units are indeed basis functions of the input variables, I, θ_o, θ_R, and $\mathbf{R}$. As such they can be linearly recombined to generate any nonlinear function of these variables and, in particular, a saccadic motor command consistent with the instruction, the current position, and the orientation of the object. This is precisely what is done at the next stage.

The output layer of the network is a 20×20 retinotopic map encoding the intended saccadic eye movement. It provides a simplified model of the motor map found in the superior colliculus, a structure that is known to be involved in the control of saccadic eye movements. The weights of the connections from the parietal/premotor maps to the output map were set by hand as follows.

The intermediate maps in the intermediate layers belong to two categories, which we called "compatible" and "incompatible." The compatible maps have combinations of edge and orientation selectivity that correspond to their command selectivity. The incompatible maps have combinations of edge and orientation that do not correspond to their command selectivity. For example, if an object is rotated by 90° counterclockwise, its top edge corresponds to the right part of the object. If a cell preferring a top edge and an object orientation of 180° is amplified by the command "go to the right," it is compatible and should contribute to activate a saccade to this location. On the other hand, if this cell prefers the command "go to the left," it is incompatible and should inhibit a saccade to this location.

Accordingly, each unit in the basis function layer sends a connection to the unit at the same retinotopic position in the output layer. The weight of that connection is set to 1 if the basis function unit belongs to a compatible map, or to −0.25 if it belongs to an incompatible map.

$$o_{ij} = \left[\sum_{k,l \text{ compatible}} P_{ij}^{k,l} - 0.25 \sum_{k,l \text{ incompatible}} P_{ij}^{k,l} \right]^{+} \quad (15)$$

The position of the peak of activity on the output map is interpreted as the endpoint of the saccade computed by the network in retinotopic coordinates. To read out the position of this peak we use a center of mass operator:

$$(x_i, x_j) = \left(\frac{\sum_{ij} iO_{ij}}{\sum_{ij} O_{ij}}, \frac{\sum_{ij} jO_{ij}}{\sum_{ij} O_{ij}} \right). \quad (16)$$

Lesion Models

We simulated the effect of a unilateral lesion of our model to determine whether the basis function approach can account for object-centered hemineglect. These simulations relied on the assumption that basis function units are distributed between hemispheres according to their preferred retinotopic and object-centered preferences. We used contralateral gradients such that the right hemisphere mostly contained neurons with retinotopic receptive fields on the left hemiretina and a preference for the left side of objects, whereas the left hemisphere had the opposite pattern.

The gradients were implemented as follows. First, each basis function map was copied twice, with one copy assigned to each hemisphere. Then, the activity of the basis function unit in each hemisphere was modulated by two multiplicative factors, $f_r(i, j)$ and $f_o(k, l)$. These factors depended, respectively, on the preferred retinotopic location i, j and the object-centered preference of the unit as specified by its preferred relative retinotopic location k and object orientation l (see below for why each pair of values k, l is uniquely associated with a particular side of the object). These factors are specific to each hemisphere and will therefore be noted as $f_r^{\text{side}}(i, j)$ and $f_o^{\text{side}}(k, l)$ where "side" can take the value "left" or "right."

$$(P_{ij}^{k,l,m})^{side} = f_r^{side}(i,j)\, f_o^{side}(k,l) P_{ij}^{k,l,m}, \quad (17)$$

where $P_{ij}^{k,l,m}$ is defined in Equation 14. In the left hemisphere, the retinotopic factor was chosen to follow a linear function of the horizontal retinotopic position of the response field, increasing from left ($i = 0$) to right ($i = 20$).

$$f_r^{left}(i,j) = \frac{1}{20} i \quad (18)$$

The reverse gradient was used in the right hemisphere.

The object-centered factor relied on the following property. As we have seen in the Experimental Procedures, each of the basis function maps is characterized by a pair of preferred object orientation and a preferred relative retinal position. Any pair of values corresponds to a particular object-centered location. For instance, the upper edge in retinal coordinates corresponds to the right side in object-centered coordinates when the object is rotated 90° counterclockwise. Accordingly, it is possible to label any of the basis function maps by its preferred object-centered location, even though basis function units do not have invariant object-centered tuning curves. The object-centered gradient was implemented by setting the factor f_o^{side} to 0.2 for units preferring the ipsilateral side of objects and 1 otherwise. For example, in the left hemisphere:

$$f_o^{left}(k,l) = \begin{cases} 0.2 & \text{if } k,l \text{ specify left side} \\ 1 & \text{otherwise} \end{cases}. \quad (19)$$

A lesion was then simulated by removing all the maps corresponding to one hemisphere and testing the reduced network with various commands, object positions, and orientations.

Acknowledgments

We thank Jon Driver, Carl Olson, and Flip Sabes for their comments and feedback on this work. A.P. and S.D. were supported by an NIH grant (MH57823-05), a fellowship from the Sloan Foundation, and a young investigator award from ONR (N00014-00-1-0642).

Received: April 23, 2002
Revised: November 4, 2002

References

Andersen, R.A., Bracewell, R.M., Barash, S., Gnadt, J.W., and Fogassi, L. (1990). Eye position effect on visual memory and saccade-related activity in areas LIP and 7a of macaque. J. Neurosci. *10*, 1176–1196.

Behrmann, M., and Moscovitch, M. (1994). Object-centered neglect in patients with unilateral neglect: effects of left-right coordinates of objects. J. Cogn. Neurosci. *6*, 151–155.

Behrmann, M., and Tipper, S.P. (1999). Attention accesses multiple reference frames: evidence from visual neglect. J. Exp. Psychol. Hum. Percept. Perform. *25*, 83–101.

Ben Hamed, S., Duhamel, J.R., Bremmer, F., and Graf, W. (2001). Representation of the visual field in the lateral intraparietal area of macaque monkeys: a quantitative receptive field analysis. Exp. Brain Res. *140*, 127–144.

Bishop, C.M. 1995. Neural Networks for Pattern Recognition (Oxford: Oxford University Press).

Boussaoud, D., Barth, T., and Wise, S. (1993). Effects of gaze on apparent visual responses of frontal cortex neurons. Exp. Brain Res. *93*, 423–434.

Deneve, S., and Pouget, A. 1998. Neural basis of object-centered representations. In Advances in Neural Information Processing Systems, M. Jordan, M. Kearns, S. Solla, eds. (Cambridge, MA: MIT Press).

Deneve, S., Latham, P., and Pouget, A. (2001). Efficient computation and cue integration with noisy population codes. Nat. Neurosci. *4*, 826–831.

Drain, M., and Reuter-Lorenz, P.A. (1997). Object-centered neglect for letters: do informational asymmetries play a role? Neuropsychologia *35*, 445–456.

Driver, J., and Pouget, A. (2000). Object-centered visual neglect, or relative egocentric neglect? J. Cogn. Neurosci. *12*, 542–545.

Driver, J., Baylis, G.C., Goodrich, S.J., and Rafal, R.D. (1994). Axis-based neglect of visual shapes. Neuropsychologia *32*, 1353–1365.

Duhamel, J., Bremmer, F., BenHamed, S., and Graf, W. (1997). Spatial invariance of visual receptive fields in parietal cortex neurons. Nature *389*, 845–848.

Duncan, J. (1984). Selective attention and the organization of visual information. J. Exp. Psychol. Gen. *113*, 501–517.

Farah, M.J., Brunn, J.L., Wong, A.B., Wallace, M.A., and Carpenter, P.A. (1990). Frames of reference for allocating attention to space: evidence from the neglect syndrome. Neuropsychologia *28*, 335–347.

Galletti, C., Battaglini, P.P., and Fattori, P. (1993). Parietal neurons encoding spatial locations in craniotopic coordinates. Exp. Brain Res. *96*, 221–229.

Gershon, E.D., Wiener, M.C., Latham, P.E., and Richmond, B.J. (1998). Coding strategies in monkey V1 and inferior temporal cortices. J. Neurophysiol. *79*, 1135–1144.

Gibson, B.S., and Egeth, H. (1994). Inhibition of return to object-

based and environment-based locations. Percept. Psychophys. *55*, 323–339.

Gottlieb, J., Kusunoki, M., and Goldberg, M. (1998). The representation of visual salience in monkey parietal cortex. Nature *391*, 481–484.

Kahneman, D., Treisman, A.M., and Gibbs, B.J. (1992). The reviewing of object files: object-specific integration of information. Cognit. Psychol. *24*, 175–219.

Lagae, L., Maes, H., Raiguel, S., Xiao, D.K., and Orban, G.A. (1994). Responses of macaque STS neurons to optic flow components: a comparison of areas MT and MST. J. Neurophysiol. *71*, 1597–1626.

Logothetis, N.K., and Pauls, J. (1995). Psychophysical and physiological evidence for viewer-centered object representations in the primate. Cereb. Cortex *5*, 270–288.

Logothetis, N.K., Pauls, J., and Poggio, T. (1995). Shape representation in the inferior temporal cortex of monkeys. Curr. Opin. Neurobiol. *5*, 522–563.

Marr, D. 1982. Vision (Cambridge, MA: MIT Press).

Marshall, J.C., and Halligan, P.W. (1993). Visuo-spatial neglect: a new copying test to assess perceptual parsing. J. Neurol. *240*, 37–40.

Moody, J., and Darken, C. (1989). Fast learning in networks of locally-tuned processing units. Neural Comput. *1*, 281–294.

Mozer, M. (1999). Explaining object-based deficits in unilateral neglect without object-based frames of reference. Prog. Brain Res. *121*, 99–119.

Olshausen, B., Anderson, C., and Essen, D.V. (1995). A multiscale dynamic routing circuit for forming size- and position-invariant object representations. J. Comput. Neurosci. *2*, 45–62.

Olson, C.R., and Gettner, S.N. (1995). Object-centered direction selectivity in the macaque supplementary eye field. Science *269*, 985–988.

Poggio, T. (1990). A theory of how the brain might work. Cold Spring Harb. Symp. Quant. Biol. *55*, 899–910.

Pouget, A., and Sejnowski, T. (1997). Spatial transformations in the parietal cortex using basis functions. J. Cogn. Neurosci. *9*, 222–237.

Pouget, A., and Sejnowski, T.J. (2001). Simulating a lesion in a basis function model of spatial representations: comparison with hemineglect. Psychol. Rev. *108*, 653–673.

Pouget, A., and Snyder, L. (2000). Computational approaches to sensorimotor transformations. Nat. Neurosci. *3*, 1192–1198.

Pouget, A., Deneve, S., and Sejnowski, T. (1999). Frames of reference in hemineglect: a computational approach. Prog. Brain Res. *121*, 81–97.

Reuter-Lorenz, P.A., Drain, M., and Hardy-Morais, C. (1996). Object-centered attentional biases in the intact brain. J. Cogn. Neurosci. *8*, 540–550.

Riesenhuber, M., and Poggio, T. (1999). Hierarchical models of object recognition in cortex. Nat. Neurosci. *2*, 1019–1025.

Sabes, P.N., Breznen, B., and Andersen, R.A. (2002). Parietal representation of object-based saccades. J. Neurophysiol. *88*, 1815–1829.

Sakata, H., Taira, M., Kusunoki, M., Murata, A., Tanaka, Y., and Tsutsui, K. (1998). Neural coding of 3D features of objects for hand action in the parietal cortex of the monkey. Philos. Trans. R. Soc. Lond. B Biol. Sci. *353*, 1363–1373.

Salinas, E., and Abbot, L. (1995). Transfer of coded information from sensory to motor networks. J. Neurosci. *15*, 6461–6474.

Schlag, J., and Schlag-Rey, M. (1987). Evidence for a supplementary eye field. J. Neurophysiol. *57*, 179–200.

Tipper, S.P., and Behrmann, M. (1996). Object-centered not scene-based visual neglect. J. Exp. Psychol. Hum. Percept. Perform. *22*, 1261–1278.

Tipper, S.P., Weaver, B., Jerreat, L.M., and Burak, A.L. (1994). Object-based and environment based inhibition of return of visual attention. J. Exp. Psychol. Hum. Percept. Perform. *20*, 478–499.

Tolhurst, D., Movshon, J., and Dean, A. (1982). The statistical reliability of signals in single neurons in cat and monkey visual cortex. Vision Res. *23*, 775–785.

Tootell, R.B., Mendola, J.D., Hadjikhani, N.K., Liu, A.K., and Dale, A.M. (1998). The representation of the ipsilateral visual field in human cerebral cortex. Proc. Natl. Acad. Sci. USA *95*, 818–824.

Wachsmuth, E., Oram, M.W., and Perrett, D.I. (1994). Recognition of objects and their component parts: response of single units in the temporal cortex of the macaque. Cereb. Cortex *4*, 509–522.

Zhou, H., Friedman, H.S., and von der Heydt, R. (2000). Coding of border ownership in monkey visual cortex. J. Neurosci. *20*, 6594–6611.